IN THE UNITED STATES PATENT AND TRADEMARK OFFICE

In re PATENT APPLICATION of

MATSUI et al. Attorney Docket No.: 11059/002001

Serial No. 09/369,735 Art Unit: 1652

Filed: August 6, 1999 Examiner: MONSHIPOURI, MARYAM

For: Methods for making and using a thermophilic enzyme as aβ-glycosidase

DECLARATION PURSUANT TO 37 C.F.R.1.132

I, Ikuo Matsui, of 1-18-45 Ninomiya, Tsukuba-shi, Ibaraki-ken, Japan, do hereby declare as follows:

1. I received my bachelor degree from the Department of Agricultural Chemistry, Faculty of Agriculture, at Sizuoka University in March 1977. I finished my doctoral course in March 1985. Since April 1985, I have been employed by the National Institute of Advanced Industrial Science and Technology (AIST), and have been conducting research in the field of biochemistry.

2. I am an inventor of the invention described and claimed in U.S. Patent Application No. 09/369,735. I have reviewed the Final Office Action mailed June 18, 2004. I have full knowledge of the present invention and cited references.

3. In order to show the differences between the subject matter of the references and the subject matter of the above-identified application, the following article, which I have authored, "Novel substrate specificity of a membrane-bound β-glycosidase from hyper thermophilic archaeon *Pyrococcus horikoshii*", FEBS Letters 467 (2000), 195-200, is attached hereto as Appendix A.

The β-glycosidase as set forth by the above-identified application has a novel substrate specificity with kcat/Km values high enough for hydrolysis of β-glycosides with long alkyl chain at the reducing end (see, e.g., page 19, lines 11-12 of the specification). The β-glycosidase of the invention also exerts its enzyme activity even at high temperatures and maintains the stability in organic solvents (See, e.g., Figure 2, and page 21, line 6).

Table 2 of Appendix A clearly shows that the subject specificity of the β-glycosidase of the invention is completely different from that of a similar β-glycosidase from another hyper thermophilic archaeon, *Sulfolobuss solfataricusis*. No other β-glycosidase having the substrate specificity as that of the β-glycosidase disclosed and claimed in the above identified application has been reported. This substrate specificity demonstrates that the β-glycosidase

of the invention, disclosed and claimed in the above-identified application, has novel characteristics that, prior to the invention, were not suspected or known and thus could not reasonably be expected to be assayed or determined by one of skill in the art of biochemistry by commonly used assay techniques as suggested in the Final Office Action.

The position stated in the Final Office Action that by examining the amino acid sequence on of skill in the art would readily know the substrate specificity and the membrane domain is incorrect.

First, one of skill in the art would not expect a β-glycosidase to have the substrate specificity described and claimed in the above-identified application. Second, based upon teachings in the art, the mere review of an amino acid sequence would not necessarily teach or suggest a membrane-binding (MB) domain. In support I submit another article by Andersson et al. ("A revised model of the active site of alternative oxidase", FEBS Letters 449 (1999), 17-22). Andersson et al. shows that the membrane-binding (MB) domain cannot be predicted from the amino acid sequence (see 2nd paragraph in the left column on page 21).

Kawarabayasi et al. discloses the genome sequence of *Pyrococcus horikoshii*. Kawarabayasi et al. do not teach or suggest a purified protein, any functional (e.g. substrate specificity) or structural characteristics of the *P. horikoshii* β-glycosidase. Thus, the position relied upon in the Final Office Action is misplaced as a person skilled in the art, such as myself, would not expect (based upon the known teachings in the art) that;

(a) the β-glycosidase would have a MB domain pursuant to Andersson et al.; and

(b) would not have the substrate specificity identified by the inventors of the above-identified application.

These characteristics could not be known without first purifying the β-glycosidase and could not be gleaned from the amino acid sequence itself. As described above, there are many characteristics that cannot be predicted from the amino acid sequence of the enzyme, even if such characteristics are inherent in the enzyme.

4. I believe that it is impossible for persons skilled in the art to forecast the characteristics of the β-glycosidase of the invention based upon the genome analysis of Kawarabayasi et al.

5. I further declare that all statements made herein of my own knowledge are true and that all statements made on information and belief are believed to be true; and further that these statements were made with the knowledge that willful false statements and the like so made are punishable by fine or imprisonment, or both, under Section 1001 of Title 18 of the United States Code and that such willful false statements may jeopardize the validity of the application or any patent issuing thereon.

Date: 6th of October , 2004

Ikuo Matsui

Ikuo Matsui

FEBS 21844 FEBS Letters 449 (1999) 17–22

A revised model of the active site of alternative oxidase

Martin E. Andersson, Pär Nordlund*

Department of Biochemistry, Stockholm University, S-106 91 Stockholm, Sweden

Received 25 January 1999; received in revised form 5 March 1999

Abstract **The plant mitochondrial protein alternative oxidase catalyses dioxygen dependent ubiquinol oxidation to yield ubiquinone and water. A structure of this protein has previously been proposed based on an assumed structural homology to the di-iron carboxylate family of proteins. However, these authors suggested the protein has a very different topology than the known structures of di-iron carboxylate proteins. We have re-examined this model and based on comparison of recent sequences and structural data on di-iron carboxylate proteins we present a new model of the alternative oxidase which allows prediction of active site residues and a possible membrane binding motif.**

Key words: Alternative oxidase; Fatty acid desaturase; Plant mitochondrion; Homology modeling; Membrane protein

1. Introduction

The di-iron carboxylate protein family has progressed from being considered an exotic member of the metalloproteins to becoming recognised as an important family of redox-active iron proteins. The number of di-iron carboxylate proteins discovered has grown in recent years and their functions as catalysts of a number of important redox reactions has been revealed. The best-studied di-iron carboxylate proteins are the R2 subunit of ribonucleotide reductase (RNR R2) [1] and the hydroxylase subunit of the soluble methane monooxygenase (MMOH) [2–7]. The reaction mechanism and molecular structure of these proteins have been studied in great detail. The active site consists of a binuclear Fe centre coordinated by two histidines and four carboxylate residues (Fig. 1A). Most of these enzymes catalyse dioxygen dependent redox reactions involving highly reactive ferryl-oxo intermediates and consequently can perform powerful chemistry including the generation of an organic radical (RNR R2) and the hydroxylation of methane to form methanol (MMOH). Other di-iron proteins of this family are the ferritins [8], stearoyl-acyl carrier protein Δ^9-desaturase (Δ^9-desaturase) [9,10] and rubrerythrin [11,12], for which structural data are available. Sequence comparisons suggest some additional hydrocarbon hydroxylases to be members of this group [13].

The di-iron carboxylate proteins can be divided into two groups (in SCOP classification termed 'RNR R2-like proteins' and 'ferritin-like proteins'), which all share a central four-helix bundle providing the carboxylate dominated first ligand sphere to the Fe centre. Among the RNR R2-like proteins, virtually no sequence homology exists, with the only similarity being the occurrence of an EXXH motif on both the second and fourth helices of the bundle. The first and third helices provide the terminal carboxylate ligands and the only true characteristic of these helices is the presence of one carboxylate residue per helix. As can be seen in Fig. 1A, the two histidines both coordinate the Fe centre from the same side and the two glutamates in the EXXH motifs (E115 and E238) serve as the bridging ligands. This arrangement requires that helices 2 and 4 lie anti-parallel next to each other (Fig. 1B).

The spacing of the different ligands always follows a specific pattern characteristic to these enzymes (Fig. 2). In the four-helix bundle, the helices are arranged in two pairs. Helices 1 and 2 form one pair and helices 3 and 4 form another pair. Within these pairs the spacing between the two co-ordinating carboxylates is always around 30 amino acids. The spacing between the two helix pairs is more variable with rubrerythrin having the shortest spacing and RNR R2 from *Escherichia coli* having the longest. In rubrerythrin the connection between the helix pairs consist of just a β-strand while in RNR R2 the connecting sequence consist of two α-helices and two β-strands making up the tip of the heart-shaped structure.

The mechanism of O_2 activation is probably similar in the di-iron carboxylate proteins [13]. The starting point for the reaction is the reduced, di-ferrous form of the enzyme. The metal centre reacts readily with O_2 and this results in the formation of a di-ferric-peroxide intermediate. This peroxide intermediate has been detected in MMOH [14], RNR R2 [15,16] Δ^9-desaturase [17] and a ferritin [18]. The next step in the reaction is the formation of the ferryl species, which has only been detected in MMOH [19] where it is the methane oxidising species. In RNR R2 one proton and one electron are supplied externally via a specific proton/electron transfer pathway [20–23] to generate intermediate X, an Fe(III)-Fe(IV) species [24–28] which is the precursor to the di-ferric tyrosyl-radical species.

Among the other proteins known to contain a di-iron site, none are capable of activating molecular oxygen. Instead the metal centre is used either for O_2 transport, as in hemerythrin [29] or for phosphoryl transfer reactions, as in purple acid-phosphatase [30]. Like the ferritins, hemerythrin is a four-helix bundle but the order and direction of the helices is different from the RNR R2-like proteins [31–33]. Furthermore, in hemerythrin the ligands to the Fe centre are five His and two bridging carboxylate residues. Even though hemerythrin is a four-helix bundle the spacing of the Fe ligands is different compared to the RNR R2-like proteins. The first helix in the bundle provides one ligand while the other three helices provide two ligands each to the Fe centre. The spacing of the ligands on these three last helices are: helix 2: HXXXE, helix 3: HXXXH, and helix 4: HXXXXD.

In purple acid-phosphatase the di-iron centre is coordinated

*Corresponding author. Fax: (46) (8) 153 679.
E-mail: par@biokemi.su.se

PII: S0014-5793(99)00376-2

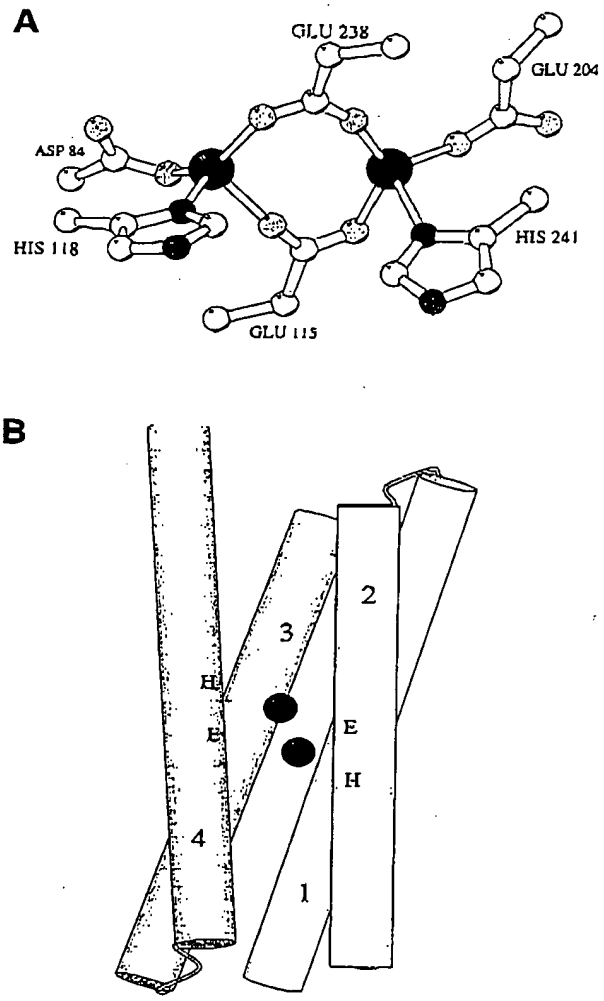

Fig. 1. A: The di-ferrous form of the iron centre in RNR R2. B: Arrangement of the helices in the four-helix bundle of the R2-type of di-iron proteins. The E and H of the two EXXH motifs are indicated. The helix numbers are placed in the N-terminal end of each helix. These figures were drawn using Molscript [54].

by 3 His, two Asp, one Asn and one Tyr [34]. The ligands to the di-iron site are provided by loops emerging from 2 β-sheets and the structure of this protein is not related to the RNR R2-like proteins.

Other metal ions can be used for the purpose of activating coordinated waters or hydroxides, eg. manganese in arginase [35]. In the crystal structure of this protein a di-Mn centre with a coordination highly similar to the RNR R2-like proteins was found [36]. The Mn-centre is coordinated by four carboxylates and two His, but this is an enzyme with α/β structure and the Mn ligands are provided by loops between a central β-sheet and the surrounding helices.

Consequently, several structural motifs exist which can accommodate a di-nuclear metal centre, but all of the proteins with known structures containing the EXXH motifs have the same fold of the central four-helix bundle. No other known protein folds containing a di-metal centre has an EXXH motif in the ligation sphere of the metal site.

2. Alternative oxidase

In the mitochondria of plants, fungi, yeast, and trypanosomes the respiratory chain has an additional protein, in addition to cytochrome *c* oxidase, that can act as the terminal electron acceptor [37]. The substrates of this 'alternative oxidase' (AOX) are ubiquinol and dioxygen, which are converted to ubiquinone and water respectively [38,39]. Respiration can thus be uncoupled from proton pumping across the matrix membrane. This enzyme was discovered as it retains catalytic activity in the presence of cyanide, a potent cytochrome *c* oxidase inhibitor [40].

Due to its strong association to the mitochondrial inner membrane, purification of the alternative oxidase has been troublesome and pure preparations of this protein have not yet been produced. Instead the biochemical work has been performed on partially purified enzyme or mitochondrial membrane fractions. There is evidence that the alternative oxidase activity requires iron [41] but the preparations of the enzyme produced to date do not show any EPR signal or absorbance above 350 nm [42]. This is unusual for a Fe protein but similar to MMOH [43] and Siedow et al. suggested in a previous modelling study that the alternative oxidase contains a di-iron centre [44,45]. In the alignments of the alternative oxidase sequences known at the time this proposal was made, three EXXH motifs were found to be conserved [44,46]. Two of these motifs were suggested to be involved in forming the di-iron centre. From proteolysis studies it was shown that the N and C-termini of the protein are on the matrix side of the membrane [47] and from hydropathy plots, two hydrophobic regions proposed to span the membrane were found [37,48]. Since the EXXH motif nearest the N-terminus is lying between the two proposed transmembrane regions, this EXXH motif was predicted to lie in the intermembrane space, hence it could not be involved in forming

	Helix 1	Helix 2		Helix 3	Helix 4
R2 *E. coli*	—D— 84 < 30 >	—E—H— 115 118	< 85 >	—E— 204 < 33 >	—E—H— 238 241
R2 *S.typhi.*	—D— 67 < 30 >	—E—H— 98 101	< 56 >	—E— 158 < 33 >	—E—H— 192 195
R2 mouse	—D— 139 < 30 >	—E—H— 170 173	< 59 >	—E— 233 < 33 >	—E—H— 267 270
MMO	—E— 114 < 29 >	—E—H— 144 147	< 61 >	—E— 209 < 33 >	—E—H— 243 246
Δ^9 desaturase	—E— 105 < 37 >	—E—H— 143 146	< 49 >	—E— 196 < 32 >	—E—H— 229 232
Bacterioferritin	—E— 18 < 32 >	—E—H— 51 54	< 39 >	—E— 94 < 32 >	—E—H— 127 130
Rubrerythrin	—E— 20 < 32 >	—E—(H)— 53 56	< 37 >	—E—E— 94 97 < 30 >	—E—H— 128 131

Fig. 2. Sequential spacing of the Fe ligands in di-iron carboxylate proteins. This list includes all proteins of this class for which an X-ray crystal structure is available. R2 *E. coli*: RNR R2 (NrdB) from *Escherichia coli* [55]. R2 *S. typhi*: RNR R2 (NrdF) from *Salmonella typhimurium* [56]. R2 mouse: RNR R2 from mouse [57]. MMO *M. capsu*: the α-subunit of the methane monooxygenase hydroxylase from *Methylococcus capsulatus* (Bath) [58]. The crystal structure of the MMO hydroxylase from *Methylosinum trichosporium* (OB3b) [59] has also been determined and the ligand numbering and spacing is identical to the *M. capsulatus* enzyme. Δ^9 desaturase: stearoyl-acyl carrier protein Δ^9-desaturase from castor (*Ricinus communis*) [10]. Bacterioferritin: bacterioferritin from *E. coli* [60]. Rubrerythrin: rubrerythrin from *Desulfovibrio vulgaris* (Hildenborough) [12].

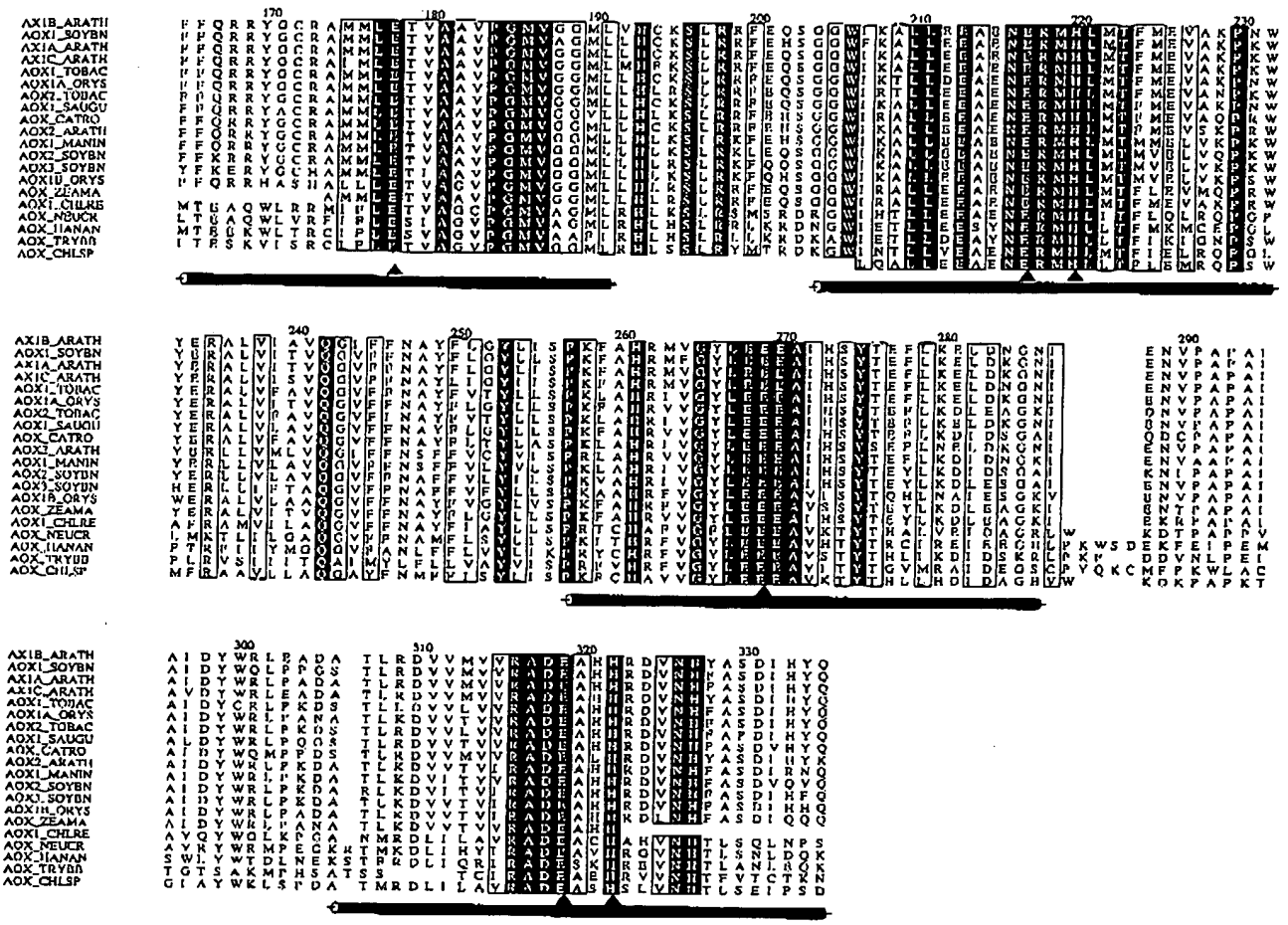

Fig. 3. Multiple sequence alignment of the most conserved region (residues 165–335, *S. guttatum* numbering) of the alternative oxidase sequences known to date. Numbering corresponds to the *S. guttatum* sequence. Arrows under the sequences correspond to the proposed Fe ligands. Black background corresponds to residues completely conserved between all species. Grey background corresponds to conservative substitutions. Abbreviations in gene names are as follows: AX and AOX: alternative oxidase; NEUCR: *Neurospora crassa*, ARATH: *Arabidopsis thaliana*; ORYS: *Oryza sativa*; CHLRE: *Chlamydomonas reinhardtii*; SAUGU: *Sauromatum guttatum*; CHLSP: *Chlamydomonas* sp.; SOYBN: soy bean (*Glycine max*); CATRO: *Catharanthus roseus*; TOBAC: tobacco plant (*Nicotiana tabacum*); HANAN: *Hunsenula anomala*; TRYBB: *Trypanosoma brucei brucei*; MANIN: *Mangifera indica*; ZEAMA: *Zea mays*.

the Fe centre, since the C-terminal part would be on the matrix side. Assuming the existence of two transmembrane helices, the authors instead used the two EXXH motifs closest to the C-terminus to build a model of the di-iron site and the central four-helix bundle inspired by the structure of MMOH and RNR R2. However, the model that was presented is not in agreement with what is known about these proteins in regards to ligand spacing and order and direction of the helices in the bundle. The helices are unusually short and the EXXH motifs appear on the first and fourth helices instead of on the second and fourth helices in the bundle. Since this proposal was made the model has been the basis for planning expression experiments, mutagenesis experiments and interpretation of data and seems to have gained acceptance as a true structure of the AOX active site. We therefore feel the need to point out weak points in this model and present an alternative model for the structure of the AOX protein.

The Siedow model suggests a di-iron site residing in a topologically and therefore evolutionarily unrelated fold to the RNR R2-like family. This is problematic from an evolutionary perspective and our doubt is further supported by additional sequence data that have recently become available, which show that one of the EXXH motifs used to build the model is not evolutionarily conserved. Meanwhile, the EXXH motif considered unlikely due to its proposed positioning in the intermembrane space, is fully conserved (Fig. 3). Based on these observations we present a new model of the alternative oxidase. This model shows how AOX could accommodate a di-iron centre within an RNR R2-like fold and further suggests possible ways of how AOX could interact with the membrane and bind the ubiquinol substrate.

3. Results and discussion

3.1. Overall structure of AOX

As the previously proposed model of the active site of the alternative oxidase [44] appears incorrect, with one of the proposed iron ligands not being conserved, we present a new structural model where only conserved residues are modelled as Fe ligands and which is consistent with an evolution-

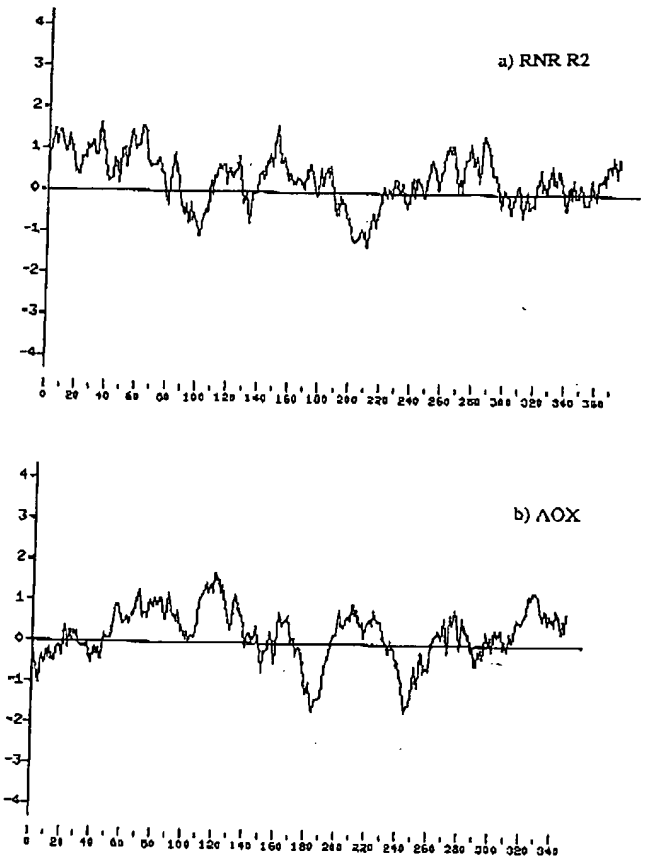

Fig. 4. Hydrophobicity plots of RNR R2 and alternative oxidase. In RNR R2 the two hydrophobic regions 85–115 and 190–230 correspond to helix C and helix E respectively. Helix C is involved in interactions forming the RNR R2 dimer and helix E is completely buried in the RNR R2 monomer surrounded by more amphiphilic helices.

ary relationship to the RNR R2-like proteins. After careful sequence comparison we decided to use the structure of the Δ^9-desaturase protein as a template for modelling the most conserved, central part of AOX. The main reason for selecting Δ^9-desaturase as a template was that the spacing of Fe ligands in the AOX sequence agrees best with that of the Δ^9-desaturase. The model, which was built using QUANTA (Molecular Simulations Inc.), consists of residues 165–335 (*Sauromatum guttatum* numbering) and covers the four-helix bundle plus the connecting region between helices 2 and 3. According to our prediction, residues 286–304 would be an insertion between helices 3 and 4, hence they were not built into the model. The assignment of the two hydrophobic regions in AOX as being transmembrane is not consistent with our model, we have therefore reevaluated the predictions of the transmembrane helices and found them not to be unambiguously predicted (using e.g. the Kyte-Doolittle method). Instead our model suggests that AOX could be an interfacial membrane protein, or that the hydrophobic helices could be involved in protein-protein interactions attaching the alternative oxidase to other membrane bound proteins. Alternatively, the hydrophobic helices could be buried, either in the core of the protein or in the dimer interface. In fact, a study conducted to map the topology of the alternative oxidase failed to conclude that the protein has a transmembrane region [47]. Comparison of hydropathy plots of the other di-iron carboxylate proteins show that helices which are completely buried within the protein can have a hydrophobicity similar to that found in the hydrophobic regions of alternative oxidase (Fig. 4). Another enlightening example of the failure to predict the structure of a membrane bound protein is that of prostaglandin H_2 synthase-1 [49]. This protein contains one stretch of sequence that was predicted to be a transmembrane helix [50] but when the crystal structure of this protein was determined it turned out that this region is not involved in membrane binding but instead is an integral part of the catalytic domain.

3.2. Model of the active site

We propose that the ligands to the Fe centre of AOX are E178, E217, H220, E269, E319 and H322 (Fig. 3). In analogy with the other di-iron proteins E217 and E319 are bridging carboxylates, while E178 and E269 are terminal ligands. This model gives spacing of sequence motifs that is more in agreement with the di-iron carboxylate proteins (Figs. 5 and 6) even though one major discrepancy still exists, the E269 residue, which gives a longer second helix pair than is normally found in di-iron proteins. One other possible Fe ligand is D283, which is conserved as D or E; however, the D283 residue is in a region of much lower conservation than E269 and is only four amino acids away from where insertions appear to have occurred making it less probable that this region is in a four-helix bundle.

On helix 3 there are three possible Fe ligands (i.e. E268, E269 or E270). Finding the correct Fe ligand among these three residues is not trivial but comparisons to the Δ^9-desaturase give some hints. On each of helices 1 and 3 of Δ^9-desaturase there are three hydrophilic residues (T104, E105 and E106 on helix 1 and Q/R195 E196 and R197 on helix 3) of which E105 and E196 are the Fe ligands. It seems that the structure can accommodate one hydrophilic residue on each side of the Fe ligand. We therefore assigned E269 as the Fe ligand of helix 3 in AOX but if E268 or E270 were to be the true Fe ligand, the main conclusions from our model would still be valid.

In all other R2-like di-iron proteins the Fe binding histidines make hydrogen bonds from the δ1 nitrogen (the nitrogen not involved in Fe binding). This is also true in our model of AOX where these hydrogen bonds are provided by residues D318 and N216 (see Fig. 7).

One disturbing property of the Siedow model, apart from the fold of the four-helix bundle, is the fact that Fe ligands are missing. There is no equivalent to E204 in R2 and the histidine corresponding to H115 is not evolutionarily conserved. In other di-iron proteins with one histidine missing, either no dinuclear metal centre is formed (as in RNR R2 H115A) or its structure is significantly perturbed (as in RNR R2 H241A)

	Helix 1		Helix 2		Helix 3		Helix 4
Alt ox. Siedow	--E--H--		--D--		--No ligands--		--E--H--
	270 273	< 9 >	283				319 322
Alt. ox. New	--E...		...E--H--		...E---		...E--H--
	178	< 38 >	217 220	< 47 >	268	< 50 >	319 322

Fig. 5. Comparison of the spacing in sequence motifs between the Siedow model and the model presented in this paper of alternative oxidase.

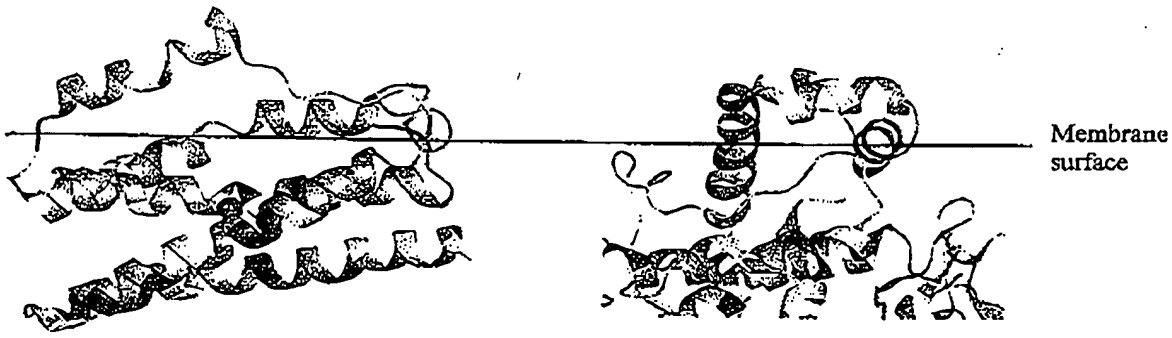

Fig. 6. Comparison of the membrane binding domain of prostaglandin H_2 synthase-1 with the proposed membrane binding domain of AOX. Grey residues are hydrophobic, yellow are hydrophilic uncharged, blue are positive, and red are negative. Note the rim of positively charged residues around the proposed membrane binding domain of AOX.

[51]. If one carboxylate and one histidine is missing the Fe centre is formed only transiently with no evidence for high-valent species being formed (as is the case in e.g. the ferritins) [52].

3.3. Ubiquinol binding site

One intriguing feature of this model is that when the sequence of the alternative oxidase is mapped onto the structure of the Δ^9-desaturase protein according to our proposed model, a hydrophobic crevice reaching down to the Fe centre is formed. This crevice is some 5 Å wide and 10 Å long and is lined by the small, conserved amino acids L177, A181, P184, G185, V187, L210, A/S214, G265, L268 and V/I272. A similar crevice is seen if RNR R2 is used as a template for model building. In this case the crevice is smaller and less hydrophobic and is lined by residues A181, P184, A/S214, H261, G265 and E268. These residues are all positioned one and two helix turns from the Fe ligands on helices 1, 2 and 3. This crevice could serve as a ubiquinol binding site and it is fairly close to two residues (corresponding to F259 and V263 in *S. guttatum* AOX) which have been proposed, from a mutagenesis screen, to be involved in ubiquinol binding in the *Arabidopsis thaliana* alternative oxidase [53].

3.4. Membrane binding domain

In the model of AOX presented here one possible membrane binding domain becomes evident. The connecting sequence between the two helix pairs (residues 236–255) is highly hydrophobic and is one of the regions predicted to be transmembrane. This connecting sequence together with the C-terminal part of helix 1 (residues 180–190) forms a hydrophobic region that could be inserted into the membrane in a manner similar to prostaglandin H2 synthase-1 (Fig. 6). This region is lined by several conserved, positively charged residues (R/H173, H193, R198, R218, K/R235 and K/R258) that could interact with the phosphate groups on the phospholipid membrane. Furthermore, the crevice we propose to be the uboquinol binding site opens up towards this hydrophobic domain which would explain how ubiquinol can access the active site of the enzyme. This is also similar to the prostaglandin H_2 synthase-1 where a substrate binding channel leads from the membrane binding domain into the active site in the catalytic domain.

However, the part of the structure connecting helices 2 and 3 in the other di-iron carboxylate proteins is normally part of the dimer interface and this could also be the case for AOX since this protein is believed to be a dimer. Several other modes for attaching the protein to the membrane, such as protein-protein interactions or a membrane binding motif in the less conserved N-terminus of the protein, are also possible.

4. Conclusions

In the present study we propose a structural model of the membrane protein alternative oxidase. This protein was previously predicted to be a di-iron carboxylate protein and a

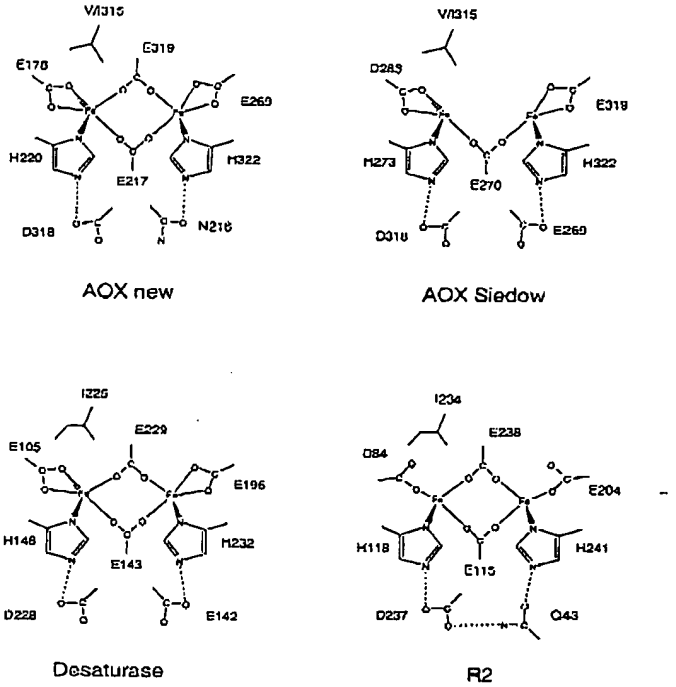

Fig. 7. Comparison of the Fe centres of the two AOX models and Δ^9-desaturase and RNR R2.

model of the active site of AOX was presented. However, this model was not in agreement with the structure of other di-iron carboxylate proteins since the order and length of the helices in the four-helix bundle was different. Our new model corresponds well with a common evolutionary origin of AOX and the di-iron carboxylate proteins since the size and order of the four helices in the bundle and the spacing of Fe ligands in the sequence is similar to di-iron carboxylate proteins. Our model is also consistent with recent sequence information on AOX since the residues we propose to be Fe ligands are completely conserved between all species. Furthermore, our model suggests that AOX is an interfacial membrane protein (or attached to the membrane via protein-protein interactions) without any transmembrane helices in analogy with prostaglandin H_2 synthase-1. This model can now be experimentally tested and used to guide mutagenesis studies to probe Fe binding and ubiquinol binding residues and allow for better planning of expression and purification efforts on this protein.

References

[1] Sjöberg, B.M. (1997) Struct. Bonding 88, 139–173.
[2] Deeth, R.J. and Dalton, H. (1998) J. Biol. Inorg. Chem. 3, 302–306.
[3] Lipscomb, J.D. and Que, L. (1998) J. Biol. Inorg. Chem. 3, 331–336.
[4] Shteinman, A.A. (1998) J. Biol. Inorg. Chem. 3, 325–330.
[5] Siegbahn, P.E.M., Crabtree, R.H. and Nordlund, P. (1998) J. Biol. Inorg. Chem. 3, 314–317.
[6] Whittington, D.A., Valentine, A.M. and Lippard, S.J. (1998) J. Biol. Inorg. Chem. 3, 307–313.
[7] Yoshizawa, K. (1998) J. Biol. Inorg. Chem. 3, 318–324.
[8] Harrison, P.M., Hempstead, P.D., Artymiuk, P.J. and Andrews, S.C. (1998) Metal Ions Biol. Syst. 35, 435–477.
[9] Fox, B.G., Shanklin, J., Ai, J., Loehr, T.M. and Sanders-Loehr, J. (1994) Biochemistry 33, 12776–12786.
[10] Lindqvist, Y., Huang, W.J., Schneider, G. and Shanklin, J. (1996) EMBO J. 15, 4081–4092.
[11] Dave, B.C., Czernuszewicz, R.S., Prickril, B.C. and Kurtz Jr., D.M. (1994) Biochemistry 33, 3572–3576.
[12] deMare, F., Kurtz, D.M. and Nordlund, P. (1996) Nature Struct. Biol. 3, 539–546.
[13] Nordlund, P. and Eklund, H. (1995) Curr. Opin. Struct. Biol. 5, 758–766.
[14] Liu, K.E., Valentine, A.M., Qui, D., Edmondson, D.E., Appelman, E.H., Spiro, T.G. and Lippard, S.J. (1995) J. Am. Chem. Soc. 117, 4997–4998.
[15] Bollinger, J.M., Krebs, C., Vicol, A., Chen, S., Ley, B.A., Edmondson, D.E. and Huynh, B.H. (1998) J. Am. Chem. Soc. 120, 1094–1095.
[16] Moënne-Loccos, P., Baldwin, J., Ley, B.A., Loehr, T.M. and Bollinger, J.M. (1998) Biochemistry 37, 14659–14663.
[17] Broadwater, J.A., Ai, J., Loehr, T.M., Sanders-Loehr, J. and Fox, B.G. (1998) Biochemistry 37, 14664–14671.
[18] Pereira, A.S., Small, W., Krebs, C., Tavares, P., Edmondson, D.E., Theil, E.C. and Huynh, B.H. (1998) Biochemistry 37, 9871–9876.
[19] Lee, S.K., Fox, B.G., Froland, W.A., Lipscomb, J.D. and Münck, E. (1993) J. Am. Chem. Soc. 115, 6450–6451.
[20] Sahlin, M., Lassmann, G., Pötsch, S., Slaby, A., Sjöberg, B.M. and Gräslund, A. (1994) J. Biol. Chem. 269, 11699–11702.
[21] Sahlin, M., Lassmann, G., Pötsch, S., Sjöberg, B.M. and Gräslund, A. (1995) J. Biol. Chem. 270, 12361–12372.
[22] Schmidt, P.P., Rova, U., Katterle, B., Thelander, L. and Gräslund, A. (1998) J. Biol. Chem. 273, 21463–21472.
[23] Parkin, S.E., Shuxian, C., Ley, B.A., Mangravite, L., Edmondson, D.E., Huynh, B.H. and Bollinger, J.M. (1998) Biochemistry 37, 1124–1130.
[24] Bollinger, J.M., Edmondson, D.E., Huynh, B.H., Filley, J., Norton, J.R. and Stubbe, J. (1991) Science 253, 292–298.
[25] Sturgeon, B.E., Burdi, D., Chen, S., Huynh, B.H., Edmondson, D.E., Stubbe, J. and Hoffman, B.M. (1996) J. Am. Chem. Soc. 118, 7551–7557.
[26] Willems, J.P., Lee, H.I., Burdi, D., Doan, P.E., Stubbe, J. and Hoffman, B.M. (1997) J. Am. Chem. Soc. 119, 9816–9824.
[27] Riggs-Gelasco, P.J., Shu, L.J., Chen, S.X., Burdi, D., Huynh, B.H., Que, L. and Stubbe, J. (1998) J. Am. Chem. Soc. 120, 849–860.
[28] Burdi, D., Willems, J.-P., Riggs-Gelasco, P., Antholine, W.E., Stubbe, J. and Hoffman, B.M. (1998) J. Am. Chem. Soc. 120, 12910–12919.
[29] Kurtz, D.M.J., Shriver, D.F. and Klotz, I.M. (1977) Coord. Chem. Rev. 20, 39–51.
[30] Klabunde, T., Strater, N., Frohlich, R., Witzel, H. and Krebs, B. (1996) J. Mol. Biol. 259, 737–748.
[31] Stenkamp, R.E., Seiker, L.C. and Jensen, L.H. (1978) J. Mol. Biol. 126, 457–466.
[32] Holmes, M.A. and Stenkamp, R.E. (1991) J. Mol. Biol. 220, 723–737.
[33] Nordlund, P. and Eklund, H. (1993) J. Mol. Biol. 232, 123–164.
[34] Strater, N., Klabunde, T., Tucker, P., Witzel, H. and Krebs, B. (1995) Science 268, 1489–1492.
[35] Reczkowski, R.S. and Ash, D.E. (1992) J. Am. Chem. Soc. 114, 10992–10994.
[36] Kanyo, Z.F., Scolnick, L.R., Ash, D.E. and Christianson, D.W. (1996) Nature 383, 554–557.
[37] Moore, A.L. and Siedow, J.N. (1991) Biochim. Biophys. Acta 1059, 121–140.
[38] Huq, S. and Palmer, J.-M. (1978) FEBS Lett. 92, 317–320.
[39] Huq, S. and Palmer, J.M. (1978) Plant Sci. Lett. 11, 351–358.
[40] Jones, M.G., Bickar, D., Wilson, M.T., Brunori, M., Colosimo, A. and Sarti, P. (1984) Biochem. J. 220, 57–66.
[41] Minagawa, N., Sakajo, S., Komiyama, T. and Yoshimoto, A. (1990) FEBS Lett. 267, 114–116.
[42] Berthold, D.A. and Siedow, J.N. (1993) Plant Physiol. 101, 113–119.
[43] Lipscomb, J.D. (1994) Annu. Rev. Microbiol. 48, 371–399.
[44] Siedow, J.N., Umbach, A.L. and Moore, A.L. (1995) FEBS Lett. 362, 10–14.
[45] Moore, A.L., Umbach, A.L. and Siedow, J.N. (1995) J. Bioenerg. Biomembr. 27, 367–377.
[46] Moore, A.L., Umbach, A.L. and Siedow, J.N. (1995) Biochem. Soc. Trans. 23, 151S.
[47] Siedow, J.N., Whelan, J., Kearns, A., Witskich, J.T. and Day, D.A. (1992) in: Molecular, Biochemical and Physiological Aspects of Plant Respiration (Lambers, H. and van der Plas, L.H.W., Eds.), pp. 19–27, SPB, The Hague.
[48] Rhoads, D.M. and McIntosh, L. (1991) Proc. Natl. Acad. Sci. USA 88, 2122–2126.
[49] Picot, D., Loll, P.J. and Garavito, R.M. (1994) Nature 367, 243–249.
[50] Merlie, J.P., Fagan, D., Mudd, J. and Needleman, P. (1988) J. Biol. Chem. 263, 3550–3553.
[51] Persson, B.O., Karlsson, M., Climent, I., Ling, J.S., Loehr, J.S., Sahlin, M. and Sjöberg, B.M. (1996) J. Biol. Inorg. Chem. 1, 247–256.
[52] Bauminger, E.R., Harrison, P.M., Hechel, D., Hodson, N.W., Nowik, I., Treffry, A. and Yewdall, S.J. (1993) Biochem. J. 296, 709–719.
[53] Berthold, D.A. (1998) Biochim. Biophys. Acta 1364, 73–83.
[54] Kraulis, P.J. (1991) J. Appl. Crystallogr. 24, 946–950.
[55] Nordlund, P., Sjöberg, B.-M. and Eklund, H. (1990) Nature 345, 593–598.
[56] Eriksson, M., Jordan, A. and Eklund, H. (1998) Biochemistry 37, 13359–13369.
[57] Kauppi, B., Nielsen, B.A., Ramaswamy, S., Larsen, I.K., Thelander, M., Thelander, L. and Eklund, H. (1996) J. Mol. Biol. 262, 706–720.
[58] Rosenzweig, A.C., Frederick, C.A., Lippard, S.J. and Nordlund, P. (1993) Nature 366, 537–543.
[59] Elango, N., Radhakrishnan, R., Froland, W.A., Wallar, B.J., Earhart, C.A., Lipscomb, J.D. and Ohlendorf, D.H. (1997) Protein Sci. 6, 556–568.
[60] Frolow, F., Kalb, A.J. and Yariv, J. (1994) Nature Struct. Biol. 1, 453–460.

Novel substrate specificity of a membrane-bound β-glycosidase from the hyperthermophilic archaeon *Pyrococcus horikoshii*

Ikuo Matsui[a,*], Yukihiro Sakai[a], Eriko Matsui[a], Hisasi Kikuchi[b], Yutaka Kawarabayasi[b], Koichi Honda[a]

[a]*National Institute of Bioscience and Human-Technology, Tsukuba, Ibaraki 305, Japan*
[b]*National Institute of Technology and Evaluation, MITI, Nishihara, Shibuyaku, Tokyo, Japan*

Received 14 December 1999; received in revised form 12 January 2000

Edited by Shozo Yamamoto

Abstract A β-glycosidase gene homolog of *Pyrococcus horikoshii* (BGPh) was successfully expressed in *Escherichia coli*. The enzyme was localized in a membrane fraction and solubilized with 2.5% Triton X-100 at 85°C for 15 min. The optimum pH was 6.0 and the optimum temperature was over 100°C, respectively. BGPh stability was dependent on the presence of Triton X-100, the enzyme's half-life at 90°C (pH 6.0) was 15 h. BGPh has a novel substrate specificity with k_{cat}/K_m values high enough for hydrolysis of β-D-Glc*p* derivatives with long alkyl chain at the reducing end and low enough for the hydrolysis of β-linked glucose dimer more hydrophilic than aryl- or alkyl-β-D-Glc*p*.

Key words: β-Glycosidase; Thermophilic archaeon; Membrane protein; Thermostable enzyme; *Pyrococcus horikoshii*

1. Introduction

The current biotechnological interest in enzymes from thermophilic microorganisms is motivated by their ability to work under conditions normally denaturing for mesophilic enzymes. Whereas conventional enzymes are irreversibly inactivated by heat, the enzymes from these extremophiles show not only great stability but also enhanced activity in the presence of common protein denaturants such as heat, detergents, organic solvents and proteolytic enzymes [1–5]. Thus, these molecules have considerable industrial potential by giving better yields under extreme operational conditions. Among the possible applications of such enzymes from thermophiles, the enzymatic synthesis of glycosides [6,7] and the saccharification of cellulotic materials by β-glycosidases have long been recognized as important and have recently received renewed attention from the pharmaceutical industry [6].

A β-glycosidase gene homolog (ORF ID: PH0366) was identified from the hyperthermophilic archaeon *Pyrococcus horikoshii* through genome sequencing [8,9]. The gene (BGPh) was successfully expressed in *Escherichia coli* and proved to be a membrane protein. The gene product was purified to homogeneity and the substrate specificity was characterized in detail. Here, we report its novel substrate specificity and enzymatic behavior as a membrane protein.

*Corresponding author. Fax: (81)-298-546151.
E-mail: ikmatsui@nibh.go.jp

Abbreviations: BGPh, β-glycosidase from *Pyrococcus horikoshii*; BMPh, a β-mannosidase gene homolog from *P. horikoshii*; BGPf, β-glucosidase from *Pyrococcus furiosus*; BMPf, β-mannosidase from *P. furiosus*; Sβ-gly, β-glycosidase from *Sulfolobus solfataricus*; IPTG, isopropyl-β-D-thiogalactopyranoside; His-BGPh, BGPh with His-tag; SDS–PAGE, sodium dodecyl sulfate–polyacrylamide gel electrophoresis; X-Glu, 5-bromo-4-chloro-3-indolyl-β-glucopyranoside; *p*-Nph-β-D-Glc*p*, *p*-nitrophenyl-β-D-glucopyranoside; LA-β-D-Glc*p*, β-D-glucopyranosides with long alkyl chains

2. Materials and methods

2.1. Chemicals

The pET-11a vector was purchased from Stratagene. The pET-15b vector and *E. coli* strain BL21(DE3) were obtained from Novagen. Vent DNA polymerase was purchased from New England Biolabs. Restriction enzymes were purchased from Promega and Toyobo (Osaka, Japan), and were used according to the manufacturers' recommendations. Ultrapure deoxynucleotide solution (dNTPs) was obtained from Pharmacia Biotech. Isopropyl-β-D-thiogalactopyranoside (IPTG) was from Takara Shuzo (Otsu, Shiga, Japan).

2.2. Cloning and expression of the gene

The genome of *P. horikoshii* was sequenced using the method of Kaneko et al. [10]. Standard cloning techniques were used throughout. The gene encoding β-glycosidase (BGPh) was amplified by the PCR method using the following two primers: TAAGAAGGAGATATACATATGCCGCTGAAATTCCCGGAAATGTTTCTCTTTGGTACC (upper primer, containing an *Nde*I site as underlined); TTTACTGCAGAGAGGATCCCTAATCCTAAAGTTGAAGTTCTGGTAG (lower primer, containing a *Bam*HI site as underlined). The PCR product was cloned into expression vectors pET-11a and pET-15b using *Nde*I and *Bam*HI sites. The resulted vectors were designated as pET-11a/BGPh and pET-15b/BGPh, respectively. The absence of additional mutations within the coding region of BGPh was verified by sequencing on an Applied Biosystems 373A DNA sequencer (Taq DyeDeoxy Terminator Cycle Sequencing kit, Perkin-Elmer).

The *E. coli* strain BL21(DE3) was transformed with the pET-11a/BGPh plasmid to express mature BGPh and pET-15b/BGPh plasmid to express His-tagged BGPh. The transformant colony was propagated in 2×YT+ampicillin medium at 37°C and was induced at $OD_{600}=1$ with 1 mM IPTG for 4 h. The induced cells were collected by centrifugation and stored at −20°C. The frozen cells (7 g) were mixed with 10 ml of 50 mM Tris–HCl buffer (pH 7.5) containing 1 mg of bovine DNase I (Sigma) and incubated at 37°C for 30 min. Triton X-100 was added to the suspension, resulting in a final concentration of 2.5%. Then, the cell suspension was heated at 85°C for 10 min and centrifuged at 5000×*g* for 20 min. The supernatant was collected and stored at 4°C.

2.3. Purification of recombinant protein

The solubilized recombinant BGPh with His-tag (His-BGPh) was subjected to affinity chromatography with Ni-conjugated Sepharose, using a stepwise elution from 5 mM to 1 M imidazole in 20 mM Tris–HCl (pH 8.0) with 0.5 M NaCl solution (His-bind Buffer kit, Novagen) containing 0.1% Triton X-100. His-BGPh was eluted with 100 mM imidazole with 0.1% Triton X-100. The enzyme samples were

0014-5793/00/$20.00
PII: S0014-5793(00)01156-X

analyzed by sodium dodecyl sulfate–polyacrylamide gel electrophoresis (SDS–PAGE) [11]; a low molecular weight electrophoresis calibration kit, purchased from Pharmacia Biotech, was also run. The purified protein demonstrated a single band with a molecular weight of 35 kDa measured on SDS–PAGE followed by Coomassie blue staining. The protein concentration was determined using a Coomassie protein assay reagent (Pierce Chemical Company). The His-tagged protein was detected with QIAexpress Detection System (Qiagen) after blotting onto a nitrocellulose membrane (Pharmacia Biotech).

2.4. Cellular localization of the activity

Localization of the BGPh activity in *E. coli* transformant cells (BL21(DE3)/pET-11a/BGPh or BL21(DE3)/pET-15b/BGPh) was examined by fractionation of the cell components. The cell membrane was isolated as follows: 7 g of the induced cells, which were frozen at −20°C, was thawed and mixed with 10 ml of 50 mM Tris–HCl buffer (pH 7.5). The cell suspension (suspension I) was sonicated with a Sonifier 250 (Branson) for 4 min at an output control level of 4 and at 30% duty cycle. The sonicated sample was centrifuged at 9000×*g* for 10 min to remove cell debris, then the supernatant (12 ml) was ultracentrifuged at 100 000×*g* for 1 h to separate the membrane fraction (1 ml) from the supernatant. The enzyme reactions were carried out at 90°C for 15 min in a solution (200 μl) containing 1.2 mM 5-bromo-4-chloro-3-indolyl-β-glucopyranoside (X-Glu) and 5 μl of each fraction, as the enzyme source, in 50 mM phosphate buffer (pH 6) with 0.3 M NaCl. After the reaction, the solution was cooled in ice and diluted with 1 ml of water; the absorbance at 620 nm was immediately measured. As a control, the assay reactions were performed under the same conditions but without X-Glu to subtract the turbidity derived from each fractionated sample.

To analyze the solubilizing effect of Triton X-100, suspension I was also heated with and without 2.5% Triton X-100 at 85°C for 10 min and the supernatant was obtained by centrifugation at 15 000×*g* for 10 min. The activity of the supernatants was measured using X-Glu as shown above.

2.5. Measurement of the kinetic parameters

The enzyme reactions were carried out at 90°C in a solution (200 μl) containing the substrate and the purified His-BGPh in 50 mM phosphate buffer (pH 6) with 0.1% Triton X-100 and 0.3 M NaCl. For the hydrolysis of *p*-nitrophenyl (*p*-Nph)-β-D-saccharides, the reaction was terminated by the addition of 1 M Na_2CO_3 (1 ml), then centrifuged at 15 000×*g* for 10 min. The concentration of the *p*-Nph group in the supernatant was quantified by measuring the absorbance at 400 nm. For the hydrolysis of β-D-glucoside, the released glucose was analyzed with a Glucose C-II Test kit (Wako Pure Chemicals, Japan). Initial velocities were obtained directly from the initial slopes of the time course plots. The K_m and k_{cat} values were calculated using the Michaelis–Menten equation and the least squares method [12]. The subsite affinity for a long alkyl chain was determined using the method reported previously [13–15] on the basis of the subsite theory [16].

2.6. Dependence on Triton X-100, optimum temperature, optimum pH and thermostability

To measure the dependence of the activity on Triton X-100, the enzyme reactions were carried out at 98°C for 20 min in 50 mM phosphate buffer (pH 6) containing Triton X-100 varying from 0.1% to 0.00002%, 3 mM *p*-Nph-β-D-glucopyranoside (*p*-Nph-β-D-Glc*p*), 57.5 pM of the purified His-BGPh and 0.1 M NaCl. Optical density measurements at A_{400} were performed as described for the enzyme assays.

The optimum temperature was measured from 50°C to 100°C in 150 mM citrate buffer (pH 5.0) without Triton X-100 and with 1 μl of heated suspension I (BL21(DE3)/pET-11a/BGPh) as enzyme source. Further details of the measurement were described in the dependence on Triton X-100.

The optimum pH was measured at 90°C in 139 mM buffer systems ranging from pH 3.9 to 5.5 in sodium acetate buffer and from 5.5 to 7.99 in phosphate buffer with 1 μl of heated suspension I (BL21(DE3)/pET-11a/BGPh or BL21(DE3)/pET-15b/BGPh). Further details of the measurement were reported in the determination of the optimum temperature.

To measure the thermostability, the His-BGPh solutions (29 nM) in 50 mM phosphate buffer (pH 6.0) containing 100 mM NaCl and 0.1% Triton X-100 were heated in sealed Eppendorf tubes at 90°C in various increments up to 24 h. The heated enzymes were assayed in phosphate buffer (pH 6.0) at 90°C as described for the determination of optimum temperature.

2.7. Sequence alignment, phylogenetic tree and hydropacy profile

Sequence alignment of β-glycosidases was performed using the GeneWorks program (IntelliGenetics) based on a PAM-250 scoring matrix. The enzymes of interest were: BGPh studied in this paper and β-mannosidase (BMPh) from *P. horikoshii* [8,9], β-glucosidase (BGPf) and β-mannosidase (BMPf) from *Pyrococcus furiosus* [17], and β-glycosidase (Sβ-gly) from *Sulfolobus solfataricus* [18]. Phylogenetic trees for the same sequences were constructed using the GeneWorks program based on the unweighted pair group method with an arithmetic mean [19]. Each hydropacy profile was analyzed with DNASIS-Mac v2.0 software based on the Kyte and Doolittle method [20].

3. Results and discussion

3.1. Localization of the activity in E. coli membrane

The intracellular localization of His-BGPh was examined (Table 1). The activity was present in the membrane fraction whereas very little activity was detected in the soluble fraction after the ultracentrifugation. The solubilizing efficiency with Triton X-100 was elevated by heating up to 85°C, whereas only 22% of the activity was extracted at room temperature. The best condition for the solubilization was 2.5% Triton X-100 at 85°C for 15 min. The native-type BGPh was also solubilized under the same condition as His-BGPh (data not shown); however, the denaturation with 8 M urea and the renaturation by direct dilution with buffer had no effect on the solubilization of the activity (data not shown).

The activity of His-BGPh was dependent on the concentration of Triton X-100. At 0.00002% Triton X-100, the activity decreased to 10% of that with 0.1% Triton X-100. Furthermore, His-BGPh was stabilized in the presence of 0.1% Triton X-100: the half-life of the activity at 90°C and pH 6.0 was 15 h. These results strongly indicate that BGPh is a thermostable membrane protein.

3.2. The substrate specificity of BGPh

For BGPh both with or without His-tag, the optimum pH was 6.0 and the optimum temperature was over 100°C. The substrate specificity of His-BGPh was examined using *p*-Nph-β-D-saccharides and β-D-glucosides as substrates. The specificity is summarized in Table 2 in comparison with that of Sβ-gly [7,21]. His-BGPh hydrolyzed aryl glycosides efficiently, showing k_{cat}/K_m values decreasing in the order *p*-Nph-β-D-Glc*p* > *p*-Nph-β-D-Gal*p* > *p*-Nph-β-D-Xyl*p* > *p*-Nph-β-D-Man*p*. β-Linked glucose dimers tested were poorly hydrolyzed; the order of preference was β1-3 > β1-4≥β1-6. The k_{cat} values of BGPh without His-tag for these β-linked glucose dimers approached 400 s^{-1}, which is comparable with those of Sβ-gly (Table 2). His-BGPh had approximately 50% of the activity of BGPh due to interference by the His-tag located at the N-terminus (data not shown). Surprisingly, the best substrates for His-BGPh were β-D-glucosides with long alkyl chains (LA-β-D-Glc*p*). The K_m values decreased according to the elongation of the alkyl chain from C_1 to C_{12}, although the k_{cat} value was constant (approximately 35 s^{-1}) for each alkyl-β-D-Glc*p*. The k_{cat} values of native-type BGPh for LA-β-D-Glc*p* approached 70 s^{-1}, calculated on the basis of the value of His-BGPh, estimating a 50% decrease in the activity from the inhibitory effect of the His-tag. The value was also appre-

Table 1
Cellular localization of the activity

Cell fractions	Activity after each treatment (A_{620})				
	Sonication	Non-heated	Heated	Non-heated with 2.5% Triton X-100	Heated with 2.5% Triton X-100
Suspension I	0.585	0.585	0.567	0.485	0.428
Supernatant at 9000×*g*	0.112	ND	ND	ND	ND
Supernatant at 15000×*g*	ND	0.008	0.005	0.107	0.255
Supernatant at 100000×*g*	0.010	ND	ND	ND	ND
Fraction precipitated at 100000×*g*	0.478	ND	ND	ND	ND

The transformant *E. coli* BL21(DE3)/pET-15b/BGPh cells were used for this experiment. The enzyme reactions were performed at 90°C and pH 6 for 15 min using X-Glu as substrate, and then A_{620} was measured as shown in Section 2.
ND: not determined.

ciable, around 30% of that of Sβ-gly (Table 2). The K_m value of His-BGPh for the hydrolysis of *n*-dodecyl-β-D-Glc*p* (alkyl chain: C_{12}) was extremely low, 30 μM at 90°C and pH 6.0. Of the substrates examined thus far, the best substrate was *n*-dodecyl-β-D-Glc*p* as shown in Table 2. The k_{cat}/K_m value of His-BGPh against *n*-dodecyl-β-D-Glc*p* was five times higher than that of *p*-Nph-β-D-Glc*p* and 870 times higher than that of laminaribiose. Even the value for *n*-octyl-β-D-Glc*p* was 0.76 times higher than that of *p*-Nph-β-D-Glc*p* and 128 times higher than that of laminaribiose. The k_{cat}/K_m value of Sβ-gly against *n*-octyl-β-D-Glc*p*, with the longest alkyl chain so far examined [21], was 0.4-fold higher than that for *p*-Nph-β-D-Glc*p* and 0.48-fold higher than that for laminaribiose. Laminaribiose and cellobiose were not good substrates for the hydrolysis of His-BGPh because of their K_m values higher than 100 mM. His-BGPh also hydrolyzed cellotriose and cellotetraose with low efficiency: the kinetic parameters were not determined because of the extremely high K_m value, whereas Sβ-gly was able to hydrolyze these oligosaccharides with high efficiency: the k_{cat}/K_m values descended in the order: cellotetraose > cellotriose > cellobiose. Thus, the substrate specificity of His-BGPh is different from those of the other β-glycosidases, including Sβ-gly [7,17,21–23]. BGPh has a novel substrate specificity with high efficiency to hydrolyze LA-β-D-Glc*p* and low efficiency to hydrolyze any β-linked glucose dimer which is more hydrophilic than aryl- or alkyl-β-D-Glc*p*. The subsite affinity ($A(C_{11})$) to bind a long alkyl chain (C_{11}) was calculated according to the following equation: $A(C_{11}) = RT\ln[(k_{cat}/K_m)$ for *n*-dodecyl-β-D-Glc*p*$/(k_{cat}/K_m)$ for methyl-β-D-Glc*p*]. The affinity was determined to be 4.26 kcal/mol. The value was reasonable when compared with the highest affinity (4.23 kcal/mol) known, that of the recognition of one glucose unit in the subsite structure of *Saccharomycopsis* amylase [13,14]. These facts indicate that the hydrophobicity of the aglycon part of the substrates is strongly recognized by the BGPh molecule and the hydrophobic substrates, including aryl- and LA-β-D-Glc*p*, are hydrolyzed effectively with low K_m values due to hydrophobic interaction between the aglycon moiety and the BGPh molecule. Thus, BGPh might be useful to synthesize novel β-glycosides, including new biosurfactants, using its transglycosylation activity because of its stability in organic solvents (data not shown).

Henrissat proposed an alternate and complementary classification scheme for glycosyl hydrolases based on amino acid sequence similarities [24–26]. For example, glycosyl hydrolase

Table 2
Comparison of the kinetic parameters between His-tagged BGPh from *P. horikoshii* and Sβ-glu from *S. solfataricus* strain MT-4 against *p*-Nph-β-D-saccharides and β-D-glucosides

Substrates	His-BGPh (90°C and pH 6.0)			Sβ-gly[a] (75°C and pH 6.5)		
	k_{cat} (s^{-1})	K_m (mM)	k_{cat}/K_m (mM^{-1} s^{-1})	k_{cat} (s^{-1})	K_m (mM)	k_{cat}/K_m (mM^{-1} s^{-1})
Laminaribiose	184	138.23	1.33	908	1.0	908.0
Cellobiose	194	1698.18	0.11	1333	30.0	44.4
Cellotriose	ND[b]	ND	ND	197	3.0	66
Cellotetraose	ND	ND	ND	584	1.7	343
β-Gentiobiose	ND	ND	ND	1360	100	14
p-Nph-β-D-Glc*p*	79	0.35	225.67	542	0.5	1084.0
p-Nph-β-D-Gal*p*	123	1.30	94.34	1020	4.7	217.0
p-Nph-β-D-Xyl*p*	3	0.10	31.83	284	4.0	71.0
p-Nph-β-D-Man*p*	2	0.14	14.60	NH[c]	NH	NH
Salicin	44	1.96	22.20	880	5.0	175.9
Methyl-β-D-Glc*p* (alkyl: C_1)	35	40.74	0.85	–[d]	–	–
n-Amyl-β-D-Glc*p* (alkyl: C_5)	31	2.02	15.11	256	1.1	232
n-Hexyl-β-D-Glc*p* (alkyl: C_6)	33	0.54	60.28	263	1.0	263
n-Octyl-β-D-Glc*p* (alkyl: C_8)	34	0.20	170.70	313	0.7	434
n-Nonyl-β-D-Glc*p* (alkyl: C_9)	39	0.08	471.57	–	–	–
n-Decyl-β-D-Glc*p* (alkyl: C_{10})	37	0.08	469.62	–	–	–
n-Undecyl-β-D-Glc*p* (alkyl: C_{11})	43	0.05	944.37	–	–	–
n-Dodecyl-β-D-Glc*p* (alkyl: C_{12})	36	0.03	1152.90	–	–	–

[a]Cited from [7,21].
[b]ND: the parameters were not determined because of too high K_m values.
[c]NH: the substrate was not hydrolyzed by Sβ-gly.
[d]–: The parameters were not reported in the references.

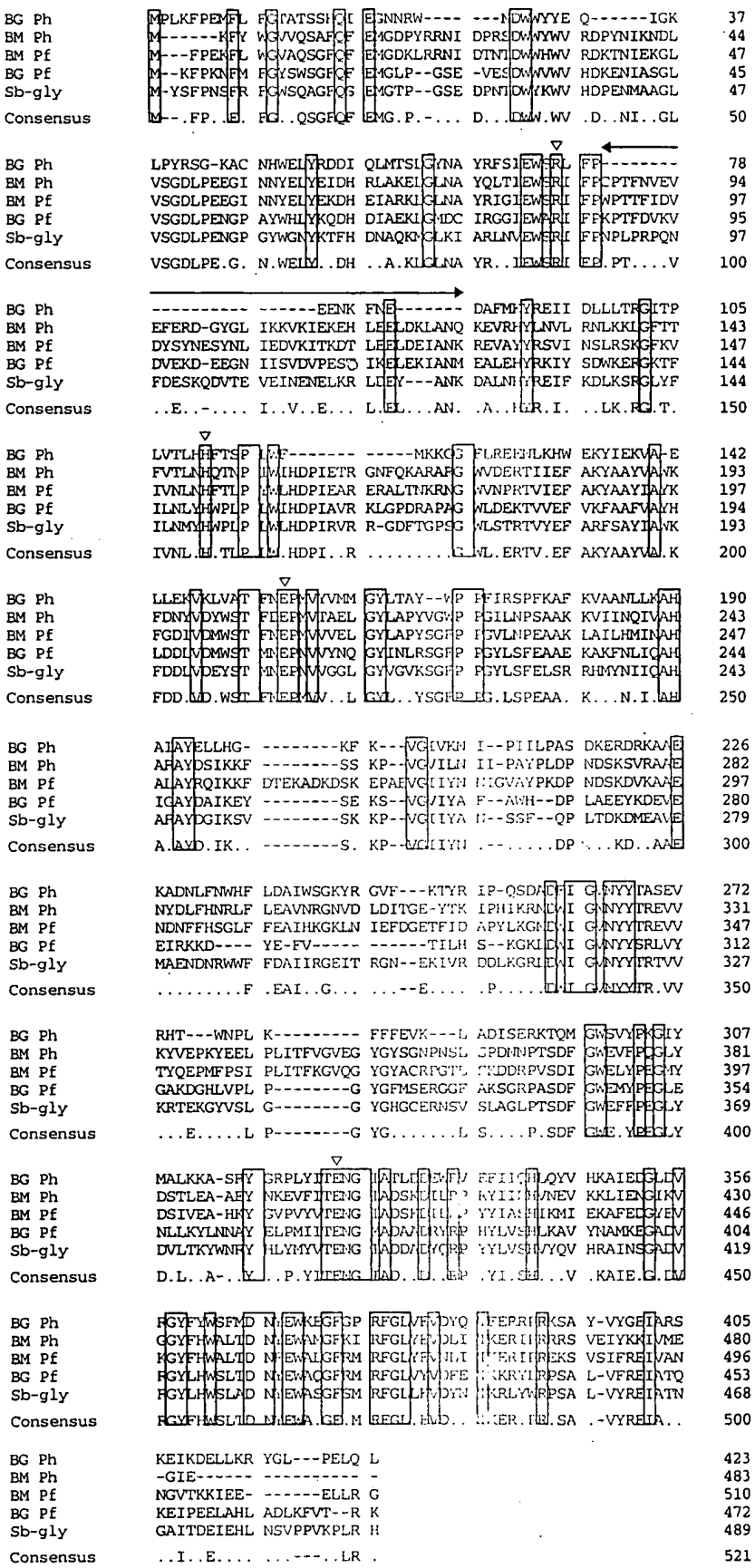
BG Ph
BM Ph
BM Pf
BG Pf
Sb-gly
Consensus

Fig. 1. Aligned amino acid sequences of five β-glycosidases from hyperthermophilic archaea. The abbreviations of the sources of the enzymes are: BGPh, β-glycosidase from *P. horikoshii*; BMPh, a β-mannosidase gene homolog from *P. horikoshii* [8,9]; BGPf, β-glucosidase from *P. furiosus* [17]; BMPf, β-mannosidase from *P. furiosus* [17]; Sβ-gly, β-glycosidase from *S. solfataricus* [18]. The conserved residues, identified automatically by the GeneWorks program, are shown in the open boxes. The reversed open triangles indicate the location of the nucleophile (E324) and the putative acid/base catalyst (E155 and H111),with R75 in the spatial proximity of the nucleophile of BGPh. The arrow shows the prominent deletion of more than 30 residues found in BGPh.
←

family 1 is composed of exo-acting, β-specific enzymes with similar amino acid sequences. The five β-glycosidases, including BGPh from the archaea domain (as shown in Fig. 1), belong to family 1. Some family 1 glycosyl hydrolases also have glycosyl transferase activities. The *S. solfataricus* β-glucosidase has been implicated in the glycosylation of membrane lipid components [27]. Similarly, the enzymatic analysis of BMPf predicted its possible role in the synthesis of intracellular components including protein, membrane components or other compounds [17]. Since the localization of BGPh on *E. coli* membrane strongly indicates the intimate interaction of the enzyme and lipid components, the detection of BGPh on the *Pyrococcus* cell surface using antibody against the enzyme must be done to clarify its true function in the *Pyrococcus* cell.

3.3. The structural elements responsible for membrane localization and the conservation of residues forming the active site

The sequence alignment among BGPh and four different β-glycosidases, whose biochemical characteristics have been reported [7,17,21–23], is shown in Fig. 1. According to the phylogenetic analysis based on the alignment, the tree has three branches: one corresponding to a β-glycosidase group that includes BGPf and Sβ-gly; another containing BMPh and BMPf, which were close to β-mannosidase. BGPh belongs to the third branch, located some distance from the first two branches. The polypeptide length of BGPh is also approximately 13% shorter than those of the other four β-glycosidases and might be one of the shortest sequences so far reported [8,17,18,28]. As shown in Fig. 1, the residues E155 and H111 of BGPh correspond to E206 and H150 as the putative acid/base catalyst in the Sβ-gly molecule [28,29], whose steric structure has been reported [30]. The residues E324 and R75 of BGPh correspond to E387, the nucleophile, and R79 in the spatial proximity of the nucleophile [28,29]. The complex structure of *Bacillus polymyxa* β-glycosidase with the inhibitor gluconate has been reported [31]. The BGPh residues, Q19, H111, N154, E155, Y267, E324, W362, E369 and W370, are completely conserved (Fig. 1) and correspond to the *B. polymyxa* β-glycosidase residues Q20, H121, N165, E166, Y296, E352, W398, E405 and W406, which form the intimate interaction with the inhibitor [31].

To understand the localization mechanism of BGPh to the membrane, a major structural difference between BGPh and the other soluble β-glycosidases was analyzed using the sequence alignment and the steric structure of Sβ-gly [30]. The Sβ-gly molecule has the classic $(\beta/\alpha)_8$ barrel fold first seen in the structure of triose phosphate isomerase [32]. For BGPh, the prominent deletion of more than 30 residues was found after the 78th residue, as indicated in Fig. 1. The deletion region of BGPh corresponds to loops from residues 89 to 125 of Sβ-gly, mainly shielding the helices 3 and 4 from solvent. The hydrophilic loops, which pack against the outer face of the barrel helices 3 and 4, were not present in the BGPh molecule. The increased hydrophobicity at barrel helices 3 and 4 of BGPh is also indicated by the comparison of the hydropacy plots of Sβ-gly (data not shown).

A tetrameric Sβ-gly structure has been reported, in which these loop regions were located at the four edges of regular tetragonal molecular arrangement [30]. Since BGPh as well as Sβ-gly were proved to be tetramer by gel filtration using buffer containing 0.01% Triton X-100 (data not shown), the deletion of the hydrophilic loops probably results in the exposure of helices 3 and 4 to the solvent at the four edges of the tetrameric structure. The exposed hydrophobic areas might interact with lipid components to embed the molecule in the membrane. Furthermore, the exposed hydrophobic areas may lead the hydrophobic substrates to the active site and bind them there. However, further studies using the crystallographic analysis are needed for a more definitive description of the detailed mechanism for recognition of the hydrophobic aglycone including a long alkyl-chain.

Acknowledgements: We are grateful to Emiko Yamamoto and Toshie Katakura for technical assistance.

References

[1] Woese, C.R. (1992) The Archaebacteria: Biochemistry and Biotechnology (Danson M.J., Hough, D.W. and Lunt, G.G., Eds.), pp. 1–10, Portland Press, London.
[2] Trincone, A., Nicolaus, B., Lama, L. and Gambacorta, A. (1993) Italian J. Chem. (Section B) 32, 25–29.
[3] Hudson, R.C., Schofield, L.R., Coolbear, T., Daniel, R.M. and Morgan, H.W. (1991) Biochem. J. 273, 645–650.
[4] Kuno, S. and Fujio, Y. (1991) J. Gen. Appl. Microbiol. 37, 25–33.
[5] Trincone, A., Dhurjati, P., Millet, J., Beguin, P. and Rossi, M. (1991) FEBS Lett. 282, 205–208.
[6] Thorson, J.S., Simon, E.S., Bednarski, M.D. and Whitesides, G.M. (1988) Tetrahedron 45, 5365–5422.
[7] Trincone, A., Improta, R., Nucci, R., Rossi, M. and Gambacorta, A. (1994) Biocatalysis 10, 195–210.
[8] Kawarabayasi, Y., Sawada, M., Horikoshi, H., Haikawa, Y., Hino, Y., Yamamoto, S., Sekine, M., Baba, S., Kosugi, H., Hosoyama, A., Nagai, Y., Sakai, M., Ogura, K., Otsuka, R., Nakazawa, H., Takamiya, M., Ohfuku, Y., Funahashi, T., Tanaka, T., Kudoh, Y., Yamazaki, J., Kushida, N., Oguchi, A., Aoki, K., Yoshizawa, T., Nakamura, Y., Robb, F.T., Horikoshi, K., Masuchi, Y., Shizuya, H. and Kikuchi, H. (1998) DNA Res. 5, 55–76.
[9] Kawarabayasi, Y., Sawada, M., Horikoshi, H., Haikawa, Y., Hino, Y., Yamamoto, S., Sekine, M., Baba, S., Kosugi, H., Hosoyama, A., Nagai, Y., Sakai, M., Ogura, K., Otsuka, R., Nakazawa, H., Takamiya, M., Ohfuku, Y., Funahashi, T., Tanaka, T., Kudoh, Y., Yamazaki, J., Kushida, N., Oguchi, A., Aoki, K., Yoshizawa, T., Nakamura, Y., Robb, F.T., Horikoshi, K., Masuchi, Y., Shizuya, H. and Kikuchi, H. (1998) DNA Res. 5, 147–155.
[10] Kaneko, T., Tanaka, A., Sato, S., Kotani, H., Sazuka, T., Miyajima, N., Sugiura, M. and Tabata, S. (1995) DNA Res. 2, 153–166.
[11] Laemmli, U.K. (1970) Nature 227, 680–682.
[12] Shimizu, M. and Hiromi, K. (1976) J. Biochem. 80, 547–555.

[13] Matsui, I., Ishikawa, K., Matsui, E., Miyairi, S., Fukui, S. and Honda, K. (1991) J. Biochem. 109, 566–569.
[14] Matsui, I., Ishikawa, K., Matsui, E., Miyairi, S., Fukui, S. and Honda, K. (1992) FEBS Lett. 310, 216–218.
[15] Suganuma, T., Matsuno, R., Ohnishi, M. and Hiromi, K. (1978) J. Biochem. 84, 293–316.
[16] Hiromi, K. (1970) Biochem. Biophys. Res. Commun. 40, 1–6.
[17] Bauer, M.W., Bylina, E.J., Swanson, R.V. and Kelly, R.M. (1996) J. Biol. Chem. 271, 23749–23755.
[18] Cubellis, M.W., Rozzo, C., Montecucch, P. and Rossi, M. (1990) Gene 94, 89–94.
[19] Nei, M. (1987) Molecular Evolutionary Genetics, pp. 293–298, Columbia University Press, New York.
[20] Kyte, J. and Doolittle, R.F. (1982) J. Mol. Biol. 157, 105–132.
[21] Nucci, R., Moracci, M., Vaccaro, C., Vespa, N. and Rossi, M. (1993) Biotechnol. Appl. Biochem. 17, 239–250.
[22] Kengen, S.W.M., Luesink, E.J., Stams, A.J.M. and Zehnder, A.J.B. (1993) Eur. J. Biochem. 213, 305–312.
[23] Bauer, M.W. and Kelly, R.M. (1998) Biochemistry 37, 17170–17178.
[24] Hen iss . B. (1991) Biochem. J. 280, 309–316.
[25] He iss . B. and Bairoch, A. (1993) Biochem. J. 293, 781–788.
[26] iss . B. and Bairoch, A. (1996) Biochem. J. 316, 695–696.
[27] an, D.W. (1991) Appl. Environ. Microbiol. 57, 1644–1649.
[28] rai . F., Barone, R., D'Auria, S., Rocci, M. and Nucci, R. hemistry 36, 3068–3075.
[29] ci. M., Trincone, A., Perugino, G., Ciaramella, M. and Ro. (1998) Biochemistry 37, 17262–17270.
[30] Ag F., Sanderson, I., Moracci, M., Ciaramella, M., Nucci, I cci, M. and Pearl, L.H. (1997) J. Mol. Biol. 271, 789–802.
[31] San- ricio, J., Hermoso, J.A., Martinez-Ripollo, M., Lequerica, nd Polaina, J. (1998) J. Mol. Biol. 275, 491–502.
[32] Ban .W., Bloomer, A.C., Petsko, G.A., Phillips, D.C., Pogson. Wilson, I.A., Corran, P.H., Furth, A.J., Milman, J.D., Off . E., Priddle, J.D. and Waley, S.G. (1975) Nature 255, 609